

1 **Quantifying the hip-ankle synergy in short-term maximal cycling**

2 Louise Burnie^{1,2,3*}; Paul Barratt⁴; Keith Davids²; Paul Worsfold^{3,5}; Jon Wheat⁶.

3 *¹Department of Sport, Exercise and Rehabilitation, Faculty of Health and Life Sciences,*
4 *Northumbria University, Newcastle upon Tyne, UK*

5 *²Sport and Physical Activity Research Centre, Sheffield Hallam University, Sheffield, UK*

6 *³Biomechanics, English Institute of Sport, Manchester, UK*

7 *⁴BAE Systems Digital, Manchester, UK*

8 *⁵Sport and Exercise Sciences, University of Chester, Chester, UK*

9 *⁶College of Health, Wellbeing and Life Sciences, Sheffield Hallam University, Sheffield, UK*

10 *Corresponding author – Louise Burnie. E-mail: louise.burnie@northumbria.ac.uk

11 T: (+44) 7801896584

12

13 Word count: 1994

14 **Abstract**

15 Simulation studies have demonstrated that the hip and ankle joints form a task-specific
16 synergy during the downstroke in maximal cycling to enable the power produced by the hip
17 extensor muscles to be transferred to the crank. The existence of the hip-ankle synergy has
18 not been investigated experimentally. Therefore, we sought to apply a modified vector coding
19 technique to quantify the strength of the hip-ankle moment synergy in the downstroke during
20 short-term maximal cycling at a pedalling rate of 135 rpm. Twelve track sprint cyclists
21 performed 3 x 4 s seated sprints at 135 rpm, interspersed with 2 x 4 s seated sprints at 60 rpm
22 on an isokinetic ergometer. Data from the 60 rpm sprints were not analysed in this study.
23 Joint moments were calculated via inverse dynamics, using pedal forces and limb kinematics.
24 The hip-ankle moment synergy was quantified using a modified vector coding method.
25 Results showed, for 28.8% of the downstroke the hip and ankle moments were in-phase,
26 demonstrating the hip and ankle joints tend to work in synergy in the downstroke, providing
27 some support findings from simulation studies of cycling. At a pedalling rate of 135 rpm the
28 hip-phase was most frequent (42.5%) significantly differing from the in- ($P = 0.044$), anti- (P
29 < 0.001), and ankle-phases ($P = 0.004$), demonstrating hip-dominant action. We believe this
30 method shows promise to answer research questions on the relative strength of the hip-ankle
31 synergy between different cycling conditions (e.g., power output and pedalling rates).

32 **Keywords:** joint moments, movement coordination, sprint cycling, vector coding.

33 **1 Introduction**

34 The goal of short-term maximal cycling is to maximise mechanical power output delivered to
35 the crank (van Soest & Casius, 2000). To achieve this, muscle and joint actions need to be
36 coordinated to facilitate energy transfer from muscles through body segments to deliver

37 maximum effective crank force (Raasch et al., 1997). Uni-articular hip and knee extensor
38 muscles (gluteus maximus and vastii) are the primary power producers in maximal cycling
39 (Dorel et al., 2012; Martin & Nichols, 2018; Raasch et al., 1997; van Ingen Schenau et al.,
40 1992). Simulation studies have demonstrated that hip extensor muscles (gluteus maximus)
41 produce energy in the downstroke which is transferred to the limb (Fregly & Zajac, 1996;
42 Raasch et al., 1997). Additionally, ankle plantar-flexor muscles (gastrocnemius and soleus)
43 need to be co-excited with hip extensors to form a synergy to transfer this energy to the crank
44 (Dorel et al., 2012; Raasch et al., 1997). Without this co-excitation, simulations indicate that
45 energy produced by the hip extensors would simply accelerate limbs (dorsiflexing the ankle
46 and hyperextending the knee), rather than being transferred into effective crank force (Raasch
47 et al., 1997). Whereas, the knee extensors (vastii) are able to transfer most of the energy they
48 generate directly to the crank (Raasch et al., 1997). Martin and Nichols (2018) provided
49 further evidence for this functional coordination mechanism using simulated work loops.
50 They demonstrated that the ankle has a different role to knee and hip joints in maximal
51 cycling - acting to transfer - instead of maximise muscle power (Martin & Nichols, 2018).
52 However, existence of the hip-ankle synergy has not been verified experimentally. Hence,
53 developing a method to experimentally quantify the strength of this synergy in cycling
54 performance is important.

55 Vector coding can be used to quantify inter-segment, inter-joint and inter-limb coordination
56 (Bayne, 2020; Chang et al., 2008; Hamill et al., 2000; Wheat & Glazier, 2006). Vector coding
57 can identify and quantify coordination differences between-participants and movements,
58 providing insights into coordination patterns not evident from observing joint or segment
59 angle data alone (Needham et al., 2014; Wheat & Glazier, 2006). Vector coding of joint

60 moment data could, provide a useful methodology to quantify strength of hip-ankle joint
61 moment synergy in short-term maximal cycling.

62 This study aimed to apply a vector coding technique to quantify strength of hip-ankle
63 moment synergy in the downstroke during short-term maximal cycling at a pedalling rate of
64 135 rpm.

65 **2 Methods**

66 **2.1 Participants**

67 Twelve competitively experienced track sprint cyclists, at under 23 international level (5),
68 Master's international and national levels (4), or Junior national level (3) participated in this
69 study. Participants were varied in sex, age and anthropometrics (4 males and 8 females, age:
70 24.1 ± 13.8 yr, body mass: 68.2 ± 11.1 kg, height: 1.70 ± 0.07 m.), but were similar in
71 cycling performance level (flying 200 m personal best: 11.61 ± 0.90 s). Participants were
72 provided with study details and gave written informed consent. The study was approved by
73 the XXXX University XXXX Research Ethics Sub-Committee.

74 **2.2 Experimental protocol**

75 An isokinetic ergometer was set up to replicate each participant's track bicycle position.
76 Riders undertook their typical warm-up on the ergometer at self-selected pedalling rate and
77 resistance for at least 10 minutes, followed by one 4 s familiarisation sprint at 135 rpm.
78 Riders then conducted 3 x 4 s seated sprints at 135 rpm, interspersed with 2 x 4 s seated
79 sprints at 60 rpm on the isokinetic ergometer with 4 minutes recovery between efforts. A
80 pedalling rate of 135 rpm was chosen as this is representative of the pedalling rate during the
81 flying 200 m event in track cycling and within an optimal pedalling rate range for track sprint

82 cyclists (Dorel et al., 2005; Kordi et al., 2020). Data from the 60 rpm sprints were not
83 analysed in this study.

84 **Isokinetic ergometer**

85 A SRM cycle ergometer frame and flywheel (Julich, Germany) were used to construct an
86 isokinetic ergometer. The modified ergometer flywheel was driven by a 2.2-kW AC
87 induction motor (ABB Ltd, Warrington, UK), controlled by a frequency inverter equipped
88 with a braking resistor (Model: Altivar ATV312 HU22, Schneider Electric Ltd, London, UK)
89 (Burnie et al., 2020). This set-up enabled participants to start their bouts at the target
90 pedalling rate, rather than expending energy in accelerating the flywheel. The ergometer was
91 fitted with force pedals (Model ICS4, Sensix, Poitiers, France) and crank encoder (Model
92 LM13, RLS, Komenda, Slovenia), sampling data at 200 Hz.

93 **2.3 Kinematic and kinetic data acquisition**

94 Two-dimensional kinematic data of each participant's left side were recorded using a 100 Hz
95 video camera with infra-red ring lights (Model: UI-522xRE-M, IDS, Obersulm, Germany)
96 (Burnie et al., 2020). Reflective markers were placed on the pedal spindle, lateral malleolus,
97 lateral femoral condyle and greater trochanter. Kinematics and kinetics on the ergometer
98 were recorded by CrankCam software (CSER, SHU, Sheffield, UK), which synchronised the
99 camera and pedal force data and was used for data processing (Burnie et al., 2020).

100 **2.4 Data processing**

101 All kinetic and kinematic data were filtered using a Butterworth fourth order (zero lag) low
102 pass filter with a cut off frequency of 14 Hz. Instantaneous left crank power was calculated
103 from the product of the left crank torque and crank angular velocity. The average left crank

104 power was calculated by averaging the instantaneous left crank power over a complete pedal
105 revolution. Joint moments were calculated via inverse dynamics (Elftman, 1939), using pedal
106 forces, limb kinematics, and body segment parameters (de Leva, 1996). Joint extension
107 moments were defined as positive.

108 Data were analysed using a custom Matlab (R2017a, MathWorks, Cambridge, UK) script.
109 Each sprint lasted for 4 s, providing six complete crank revolutions. Joint moments were
110 resampled to 100 data points around the crank cycle and the mean value at each time point
111 was calculated to obtain a single ensemble-averaged time series for each trial. Owing to
112 technical problems for two participants only data from two instead of three sprints was
113 collected.

114 **Quantifying hip-ankle joint synergy**

115 To quantify hip-ankle joint coordination and strength of the hip-ankle joint synergy a vector
116 coding method was applied to joint moment-moment diagrams (Chang et al., 2008). These
117 were selected as the most appropriate variables to evidence if net hip and ankle joint
118 moments act in synergy during the downstroke (Fregly & Zajac, 1996). Coupling angles (γ_i)
119 were calculated from hip-ankle moment diagrams (Figure 1) for each crank cycle data point
120 for all revolutions of each participant's sprints (Chang et al., 2008). The coupling angle is
121 defined as the orientation of the vector (relative to the right horizontal) between two adjacent
122 points on the moment-moment plot, Figure 2. Since coupling angles are directional in nature,
123 mean coupling angles were computed using circular statistics (Batschelet, 1981).

124 Mean coupling angles for each participant were categorised into four coordination phases: in-
125 phase, anti-phase, hip-phase and ankle-phase based on proposals of Chang et al. (2008)
126 (Figure 2). When coupling angle values are 45° and 225° (a positive diagonal), the

127 components are in-phase: both hip and ankle moments are increasing or decreasing at similar
128 rates, i.e., hip and ankle joints are working in synergically (Arnold et al., 2017). Conversely,
129 when coupling angles are 135° and 315° (a negative diagonal), components are anti-phase.
130 For example, when hip moments are increasing whilst ankle moment are decreasing. When
131 coupling angles are parallel to the horizontal (0° and 180°), ankle moments are changing but
132 not hip moments – ankle-phase. When coupling angles are parallel to the vertical (90° and
133 270°), hip moments are changing but not ankle moments – hip-phase. Since coupling angles
134 rarely lie precisely on these angles, the unit circle was split into 45° bins used by Chang et al.
135 (2008) (Figure 2). Frequencies within which mean coupling angles lay in these coordination
136 patterns, during the downstroke (defined between crank angles of 0 to 180°) were calculated
137 for each participant, using the following equation: Frequency of coordination phase (%) =
138 $(\text{Number of occurrences of coordination phase}/51) \times 100$, (note there are 51 data points in the
139 downstroke). This process was repeated to calculate group mean coupling angles for sprints
140 at 135 rpm and coupling angle variability was calculated according to Needham et al. (2014)
141 (Figure 3). Strength of the hip-ankle synergy was quantified by the frequency of in-phase
142 coordination pattern between hip and ankle moments in the downstroke.

143 **2.5 Statistical analysis**

144 Differences between frequencies of coordination phases were assessed using a Friedman test
145 with post-hoc Wilcoxon matched pairs using IBM SPSS Statistics Version 28 (IBM UK Ltd,
146 Portsmouth, UK).

147 **3 Results**

148 Average left crank power over a complete revolution for sprints at 135 rpm was 494.1 ± 91.2
149 W. Hip and ankle moments were in-phase for 28.8% of the downstroke, with the hip-phase

150 the most frequent coordination phase (42.5%) (Figure 4). A Friedman test ($\chi^2 = 19.3$, $P <$
151 0.0005) indicated that coordination phase frequencies differed across the four coordination
152 phases. Post-hoc Wilcoxon matched pairs indicated that in-phase was significantly different
153 to anti-phase ($P = 0.004$), hip-phase ($P = 0.044$) and ankle-phase ($P = 0.017$). Hip-phase was
154 significantly different to the anti-phase ($P < 0.001$), and ankle-phase ($P = 0.004$).

155 **4 Discussion**

156 We demonstrated that a vector coding method can be used to quantify strength of hip-ankle
157 joint moment synergy during the downstroke in cycling. Data imply a tendency for hip and
158 ankle joints to work in synergy in the downstroke during short-term maximal cycling at a
159 pedalling rate of 135 rpm.

160 The evidence of in-phase coordination between the hip and ankle joints in the downstroke at
161 135 rpm, provides some support for the simulation studies suggesting that hip and ankle
162 joints need to work in synergy to transfer energy produced by hip extensors to the crank
163 (Fregly & Zajac, 1996; Raasch et al., 1997). Fregly and Zajac (1996) modelled steady state
164 pedalling at 75 rpm and Raasch et al. (1997) modelled the acceleration phase with pedalling
165 rate increasing from 80 to 120 rpm through a revolution. Our results suggest that the hip-
166 ankle synergy may not be as strong at pedalling rates higher than previously modelled. A key
167 factor that could influence the strength of the hip-ankle synergy is the time available in the
168 downstroke to coordinate joint actions. At 75 rpm the downstroke lasts 0.40 seconds
169 (pedalling rate used in Fregly and Zajac (1996) study), compared to 0.22 seconds at 135 rpm.
170 Therefore, this suggests as the task complexity increases (e.g., due to changes in pedalling
171 rate from 75 to 135 rpm), strength of hip-ankle synergy reduces, implying it is more
172 challenging to coordinate joint moments at higher pedalling rates. This observation supports

173 previous findings suggesting that, as task complexity increases, differences in coordination
174 and coordination variability emerge (Weir et al., 2019).

175 At a pedalling rate of 135 rpm, the hip-phase is the most frequent coordination phase in the
176 downstroke suggesting that sprints at 135 rpm display a hip-dominant coordination pattern. A
177 much greater contribution from hip extension power to crank power at higher pedalling rates
178 has been observed, identifying the optimal pedalling rate for maximum hip extension power
179 was around 150 rpm, whereas the optimal pedalling rate for knee extension and flexion
180 power was lower (McDaniel et al., 2014). Our finding that hip-phase coordination is
181 dominant at higher pedalling rate supports and expands upon the notion that the role of the
182 hip becomes more important at higher pedalling rates, from a power production and
183 coordination perspective.

184 This study demonstrated the application of vector coding to quantify hip-ankle moment
185 synergy in maximal cycling. Further research is required to investigate the presence of hip-
186 ankle moment synergy in the downstroke at different pedalling rates and power outputs.

187 **5 Conclusion**

188 A modified vector coding technique can be used to quantify the strength of the hip-ankle
189 moment synergy in the downstroke during cycling. Hip and ankle joints tend to work in
190 synergy in the downstroke during short-term maximal cycling, providing some support for
191 findings of previous cycling simulation studies. This method could potentially be used to
192 assess cyclists' pedalling techniques and to monitor effect of training or equipment
193 interventions on coordination patterns.

194 **6 References**

- 195 Arnold, J. B., Caravaggi, P., Fraysse, F., Thewlis, D., & Leardini, A. (2017). Movement
196 coordination patterns between the foot joints during walking. *Journal of foot and ankle*
197 *research*, 10(1), 1-7.
- 198 Batschelet, E. (1981). *Circular statistics in biology*. Academic Press.
- 199 Bayne, H., Donaldson, B., Bezodis, N. (2020). *Inter-limb coordination during sprint*
200 *acceleration* 38th International Society of Biomechanics in Sport, Online, YouTube.
- 201 Burnie, L., Barratt, P., Davids, K., Worsfold, P., & Wheat, J. (2020). Biomechanical
202 measures of short-term maximal cycling on an ergometer: A test-retest study. *Sports*
203 *biomechanics*, 1-19. <https://doi.org/10.1080/14763141.2020.1773916>
- 204 Chang, R., Van Emmerik, R., & Hamill, J. (2008). Quantifying rearfoot–forefoot
205 coordination in human walking. *Journal of Biomechanics*, 41(14), 3101-3105.
- 206 de Leva, P. (1996). Adjustments to zatsiorsky-seluyanov's segment inertia parameters.
207 *Journal of Biomechanics*, 29(9), 1223-1230.
- 208 Dorel, S., Guilhem, G., Couturier, A., & Hug, F. (2012). Adjustment of muscle coordination
209 during an all-out sprint cycling task. *Medicine and science in sports and exercise*, 44(11),
210 2154-2164. <https://doi.org/10.1249/MSS.0b013e3182625423>
- 211 Dorel, S., Hautier, C. A., Rambaud, O., Rouffet, D., Praagh, E. V., Lacour, J. R., & Bourdin,
212 M. (2005). Torque and power-velocity relationships in cycling: Relevance to track sprint
213 performance in world-class cyclists. *International Journal of Sports Medicine*, 26(9), 739-
214 746. <https://doi.org/10.1055/s-2004-830493>
- 215 Elftman, H. (1939). Forces and energy changes in the leg during walking. *American journal*
216 *of physiology*, 125(2), 339-356.
- 217 Fregly, B. J., & Zajac, F. E. (1996). A state-space analysis of mechanical energy generation,
218 absorption, and transfer during pedaling. *Journal of Biomechanics*, 29(1), 81-90.

219 Hamill, J., Haddad, J. M., & McDermott, W. J. (2000). Issues in quantifying variability from
220 a dynamical systems perspective. *Journal of Applied Biomechanics*, *16*(4), 407-418.

221 Kordi, A. M., Folland, J., Goodall, S., Menzies, C., Patel, T. S., Evans, M., Thomas, K., &
222 Howatson, G. (2020). Cycling-specific isometric resistance training improves peak power
223 output in elite sprint cyclists. *Scandinavian Journal of Medicine & Science in Sports*, *30*,
224 1594-1604.

225 Martin, J. C., & Nichols, J. A. (2018). Simulated work loops predict maximal human cycling
226 power. *Journal of Experimental Biology*, *221*(13), jeb180109.
227 <https://doi.org/10.1242/jeb.180109>

228 McDaniel, J., Behjani, N. S. E. S. J., Brown, N. A. T., & Martin, J. C. (2014). Joint-specific
229 power-pedaling rate relationships during maximal cycling. *Journal of Applied Biomechanics*,
230 *30*(3), 423-430.

231 Needham, R., Naemi, R., & Chockalingam, N. (2014). Quantifying lumbar–pelvis
232 coordination during gait using a modified vector coding technique. *Journal of Biomechanics*,
233 *47*(5), 1020-1026.

234 Raasch, C. C., Zajac, F. E., Ma, B., & Levine, W. S. (1997). Muscle coordination of
235 maximum-speed pedaling. *Journal of Biomechanics*, *30*(6), 595-602.
236 [https://doi.org/10.1016/S0021-9290\(96\)00188-1](https://doi.org/10.1016/S0021-9290(96)00188-1)

237 van Ingen Schenau, G. J., Boots, P. J. M., De Groot, G., Snackers, R. J., & van Woensel, W.
238 W. L. M. (1992). The constrained control of force and position in multi-joint movements.
239 *Neuroscience*, *46*(1), 197-207.

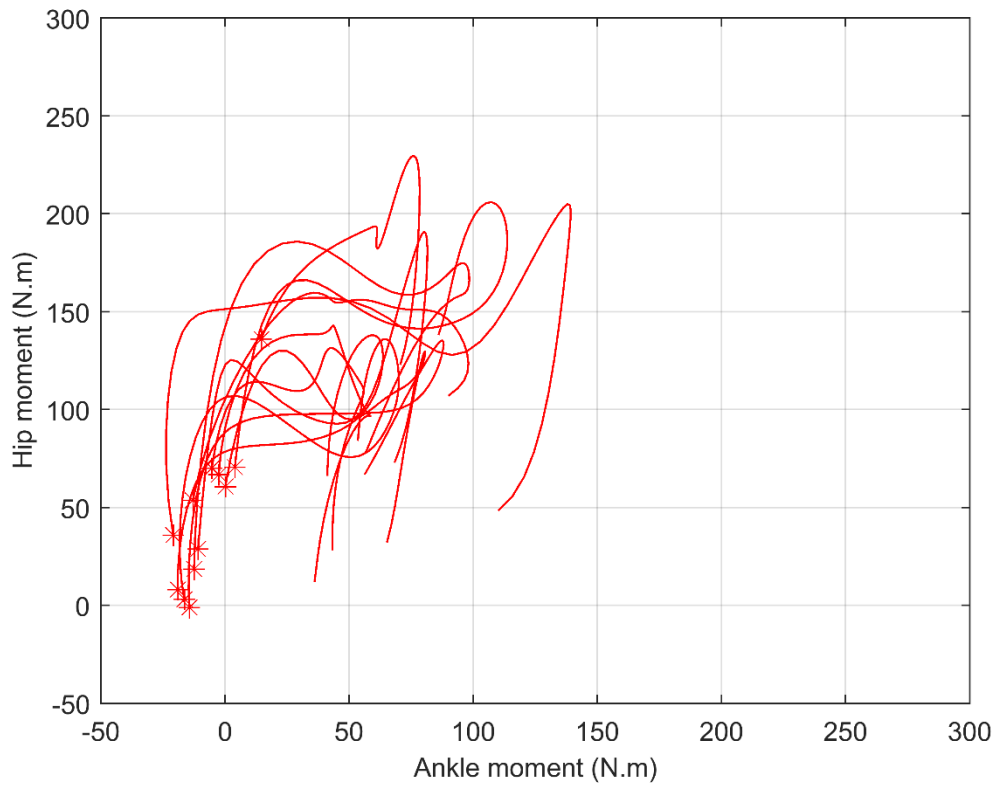
240 van Soest, A. J., & Casius, L. J. (2000). Which factors determine the optimal pedaling rate in
241 sprint cycling? *Medicine and science in sports and exercise*, *32*(11), 1927-1934.

242 Weir, G., van Emmerik, R., Jewell, C., & Hamill, J. (2019). Coordination and variability
243 during anticipated and unanticipated sidestepping. *Gait & posture*, *67*, 1-8.

244 Wheat, J., & Glazier, P. S. (2006). Chapter 9: Measuring coordination and variability in
245 coordination. In K. Davids, S. Bennett, & K. M. Newell (Eds.), *Movement system variability*
246 (pp. 167-181). Human Kinetics.

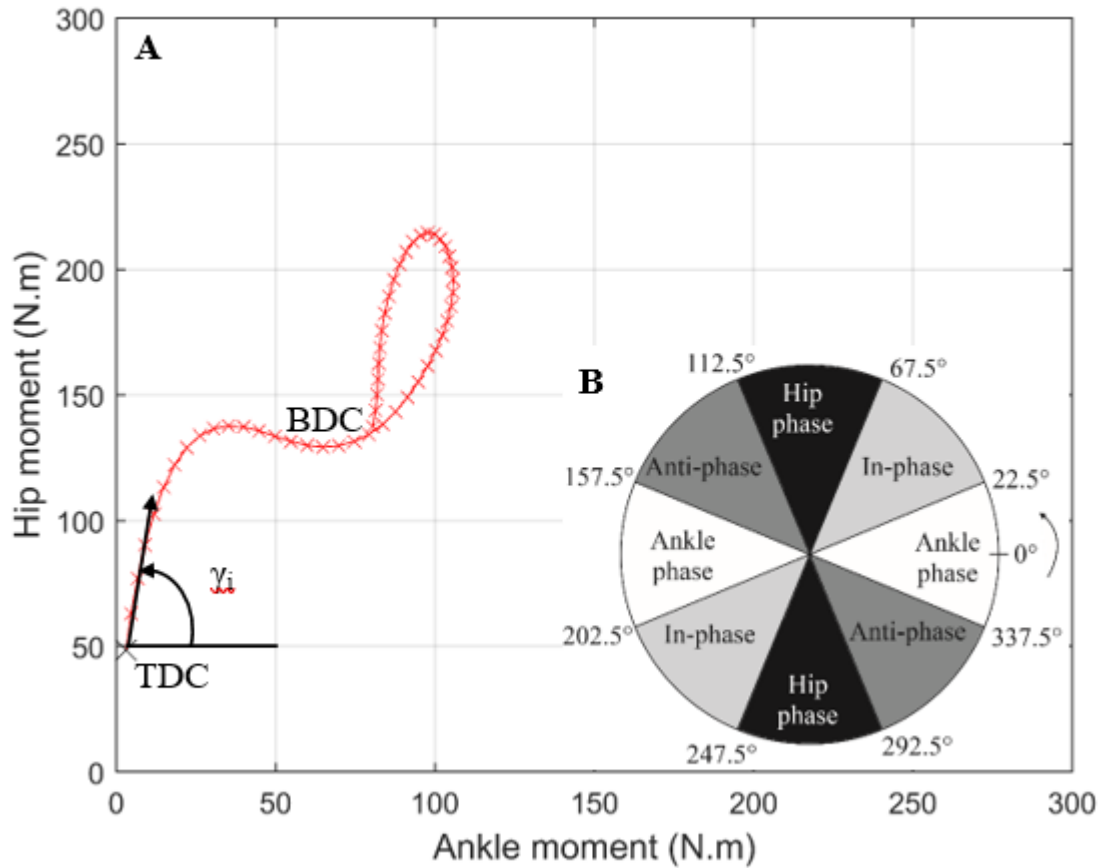
247

248 **7 Figure legends**



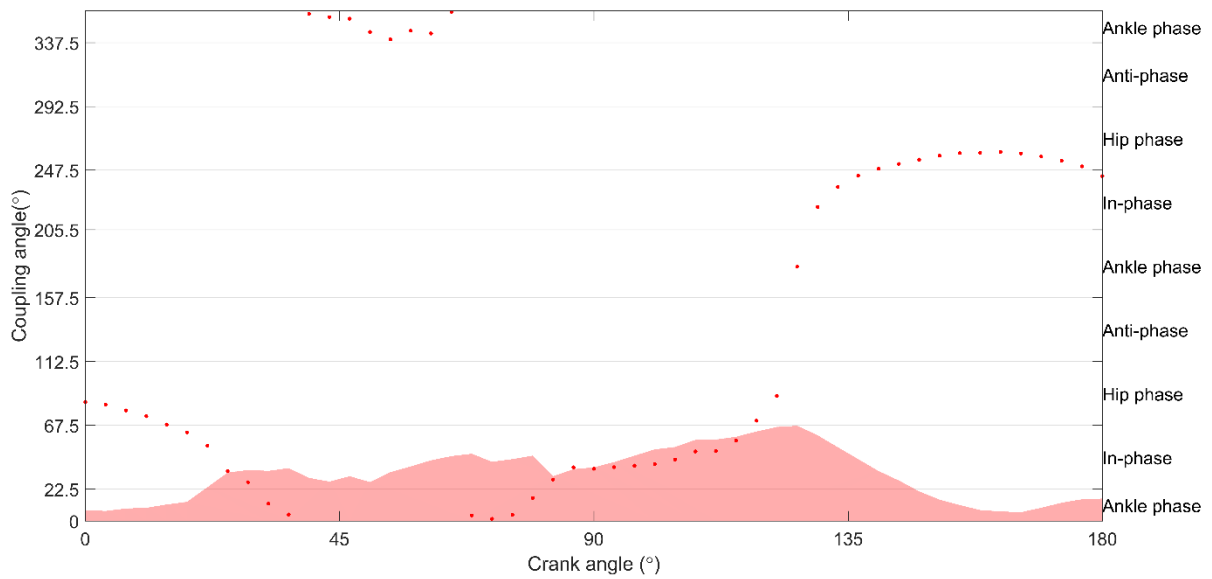
249

250 **Figure 1: Mean hip-ankle moment plots for sprints at 135 rpm for the downstroke for**
251 **each participant, with * indicating top dead centre (TDC).**



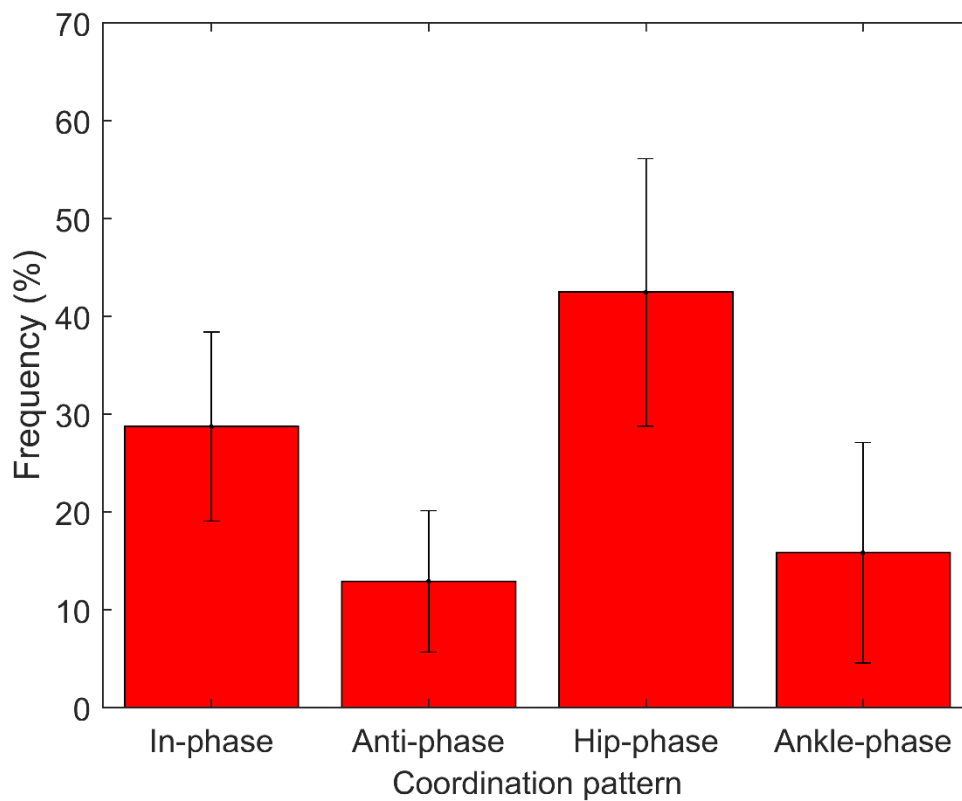
252

253 **Figure 2: A: An illustration of the calculation for a coupling angle (γ_i) from hip-ankle**
 254 **moment plot (one downstroke during a sprint). Top dead centre (TDC) = 0°, and**
 255 **bottom dead centre (BDC) = 180°. B: The coordination pattern classification system for**
 256 **the coupling angle (γ_i)**



257

258 **Figure 3: Mean coupling angle for hip-ankle moments for sprints at 135 rpm for the**
 259 **downstroke. Shaded area represents coupling angle variability.**



260

261 **Figure 4: Hip-ankle moment coordination patterns during downstroke phase of the**
 262 **crank cycle for sprints at 135 rpm.**